American Journal of Pathology, Vol. 163, No. 6, December 2003

Interference with Transforming Growth Factor-β/Smad3 Signaling Results in Accelerated Healing of Wounds in Previously Irradiated Skin

Kathleen C. Flanders,* Christopher D. Major,* Alidad Arabshahi,* Ekinadese E. Aburime,* Miya H. Okada,* Makiko Fujii,* Timothy D. Blalock,† Gregory S. Schultz,† Anastasia Sowers,‡ Mario A. Anzano,* James B. Mitchell,‡ Angelo Russo,‡ and Anita B. Roberts*

From the Laboratory of Cell Regulation and Carcinogenesis and the Radiation Oncology Branch,‡ National Cancer Institute, Bethesda, Maryland; and the Department of Obstetrics/Gynecology,† Institute of Wound Healing, University of Florida, Gainesville, Florida*

Transforming growth factor (TGF)-β regulates many aspects of wound repair including inflammation, chemotaxis, and deposition of extracellular matrix. We previously showed that epithelialization of incisional wounds is accelerated in mice null for Smad3, a key cytoplasmic mediator of TGF-β signaling. Here, we investigated the effects of loss of Smad3 on healing of wounds in skin previously exposed to ionizing radiation, in which scarring fibrosis complicates healing. Cutaneous wounds made in Smad3-null mice 6 weeks after irradiation showed decreased wound widths, enhanced epithelialization, and reduced numbers of neutrophils and myofibroblasts compared to wounds in irradiated wild-type littermates. Differences in breaking strength of wild-type and Smad3-null wounds were not significant. As shown previously for neutrophils, chemotaxis of primary dermal fibroblasts to TGF-β required Smad3, but differentiation of fibroblasts to myofibroblasts by TGF-β was independent of Smad3. Previous irradiation-enhanced induction of connective tissue growth factor mRNA in wild-type, but not Smad3-null fibroblasts, suggested that this may contribute to the heightened scarring in irradiated wild-type skin as demonstrated by Picrosirius red staining. Overall, the data suggest that attenuation of Smad3 signaling might improve the healing of wounds in previously irradiated skin commensurate with an inhibition of fibrosis. *(Am J Pathol 2003, 163:2247–2257)*

Transforming growth factor (TGF)-β regulates many cellular processes including embryogenesis, inflammation, immune responses, and tissue repair. In wound healing, diverse effects of TGF-β on the many individual participating cell types, including keratinocytes, fibroblasts, inflammatory cells, and endothelial cells, are integrated into a specific temporal sequence of events within a defined tissue architecture.[1–3] Although TGF-β is released from degranulating platelets at the time of wounding, all of the participating cells can both produce and respond to TGF-β during the course of the healing process.[4,5] TGF-β stimulates the chemotaxis of fibroblasts, neutrophils, and macrophages within the wound bed, alters the pattern of cytokine production by macrophages, and induces fibroblasts to secrete extracellular matrix proteins such as collagens and fibronectin.[1] Added exogenously to a wound, TGF-β1 can increase wound breaking strength and matrix deposition.[6–8]

TGF-β signals through transmembrane receptor serine/threonine kinases that activate a family of cytoplasmic proteins called Smads, which translocate to the nucleus to regulate expression of target genes.[9] Although Smad2 and Smad3 are each phosphorylated directly by the TGF-β type I receptor kinase, Smad3 plays a unique role in the cellular and tissue responses to wounding. Thus cutaneous wounds in Smad3-null (KO) mice show enhanced rates of epithelialization and reduced inflammation compared to wild-type (WT) littermates.[10] These findings suggested that KO mice may also display an enhanced wound healing response in compromised wounds characterized by increased inflammation, as we have shown to be characteristic of irradiated tissues.[11]

Radiation therapy and surgery are frequently combined in the clinical treatment of malignancies, such that impaired or delayed healing of wounds in irradiated tis-

K. C. F., C. D. M., and A. A. contributed equally to this work.

Accepted for publication August 4, 2003.

Present address of C. D. M.: Johnson & Johnson Pharmaceutical Research & Development, L.L.C, Drug Discovery, Spring House, PA 19477-0776.

Present address of A. A.: Division of Otolaryngology, University of Maryland School of Medicine,16 S. Eutaw St., Suite 500, Baltimore, MD 21201.

Address reprint requests to Anita B. Roberts, Laboratory of Cell Regulation and Carcinogenesis, National Cancer Institute, Building 41, Room C629, 41 Library Dr., MSC 5055, Bethesda, MD 20892-5055. E-mail: robertsa@dce41.nci.nih.gov.

sue may present clinical complications.[12,13] Models of impaired healing use irradiation of a skin flap with shielding of the rest of the animal to avoid effects on bone marrow.[14–16] Impaired healing of irradiated skin is because of, in part, toxic effects on dermal fibroblasts responsible for deposition and remodeling of the collagen matrix, resulting in decreased wound bursting strength of linear incisions.[14,17,18] TGF-β levels are increased in irradiated mouse skin[19,20] and remain elevated for long periods after irradiation in both pig and human skin.[21,22] We have shown that enhanced expression of TGF-β1 as well as epidermal hyperplasia and acanthosis seen in skin of mice after irradiation are all severely attenuated in KO mice.[11]

Based on these observations, we investigated whether loss of Smad3 would also improve the healing of radiation-impaired wounds. We show that the acute tissue response to irradiation is markedly attenuated in KO mice and that incisional wounds made in skin 6 weeks after irradiation are narrower and show an increased rate of epithelialization and reduced inflammatory cell infiltrate compared to WT littermate controls. Reduced expression of connective tissue growth factor (CTGF) both *in vivo* and *in vitro* may contribute to the reduced scarring in KO mice. These data implicate Smad3 as a potential target of therapeutic intervention in the healing of compromised wounds.

Materials and Methods

Mouse Model

KO (*Smad3*$^{ex8/ex8}$) mice were generated by targeted disruption of the Smad3 gene by homologous recombination.[23] Genotyping was done by polymerase chain reaction analysis of tail DNA.

Irradiation of Smad3 Mice

Local irradiation (30 or 45 Gy) of flank skin of WT heterozygous (HT), and KO littermates (5 to 6 weeks of age) was performed as described.[11] For some experiments, both flanks were irradiated, for others one side was sham-irradiated and served as a nonirradiated control. Protocols for irradiation and wounding were approved by the National Cancer Institute Animal Care and Use Committee.

Cutaneous Wounding Protocol

Six weeks after irradiation (30 Gy), mice were anesthetized and 1-cm linear incisions were made through the skin and panniculus carnosus muscle within the irradiated region. At 1 to 5 days or 5 weeks after wounding, mice were euthanized and wounds excised, fixed in 10% buffered neutral formalin for 18 hours, and transferred to 70% ethanol before paraffin embedding and sectioning (5 μm sections through the center of the wound).

Quantitation of Wound Histology and Cellularity

Hemotoxylin and eosin-stained sections were analyzed using a Zeiss Axioplan microscope equipped with an MTI CCD camera (Dage, Michigan City, IN) in conjunction with Image Pro-Plus Version 2.0 software. Epithelial migration was determined by tracing the epithelial advancement from the wound edge. Wound width represents the linear distance between the margins of the wound. Wound closure (percent epithelialization) is the distance of epithelial migration divided by the wound width. Cells were counted in three $\times$400 magnification fields in the wound bed in 12 sections of each genotype. Mast cells, macrophages, and myofibroblasts were identified as described.[11] Neutrophils were visualized by immunohistochemical staining with rat anti-mouse neutrophil antibody (Serotec, Raleigh, NC) at 0.5 μg/ml. Isotype-matched normal IgG at the same concentration as the primary antibody was used as a negative control.

To analyze the collagen content and architecture of irradiated skin, deparaffinized sections were stained for 1 hour with a 0.1% solution of Sirius red F3BA (Chroma-Gesellschaft, Munster, Germany) in saturated aqueous picric acid, washed in 0.01 N HCl, and viewed under polarized light. Images representing 70,000-μm^2 areas of dermis within or on either side of the wound bed were analyzed by quantifying pixels representing strong orange/red birefringence and weak yellow/green birefringence. The ratio of orange/red to yellow/green pixels is referred to as the scar index with a higher number representing increased fibrosis. Results are expressed as mean $\pm$ SEM. Significant intergroup differences were determined by applying the two-sample assuming unequal variance *t*-test.

Analysis of Gene Expression by Immunohistochemistry

Immunolocalization of extracellular TGF-β1 using the antibody CC 1-30-1 (1 μg/ml) was performed as described.[11] CTGF was detected using an affinity-purified goat anti-human CTGF antibody.[24] For CTGF staining deparaffinized sections were blocked with Tris-buffered saline and 10% rabbit serum and incubated overnight at 4°C with the primary antibody (14 μg/ml) in blocking buffer. Sections were washed, incubated with biotinylated rabbit anti-goat IgG, washed again, incubated with alkaline phosphatase-conjugated streptavidin followed by Vector Red alkaline phosphatase visualization substrate (Vector Laboratories, Burlingame CA), and photographed under bright-field illumination. Negative controls, which included replacing primary antibody with antibody plus blocking peptide or with normal IgG, showed no staining.

Cell Culture and Treatment

WT and KO dermal fibroblasts were isolated and cultured as described.[11] For examination of differentiation to myofibroblasts, fibroblasts (passages 1 to 3) were cultured in

DMEM/ITS + 1 (Sigma Chemical Co., St. Louis, MO)/1% Pen-Strep in the presence or absence of 5 ng/ml of TGF-β1, which was replaced on day 2. Cells were rinsed and scraped into RIPA buffer for Western blot analysis on day 4. For analysis of RNA expression, cells were grown in media containing 10% serum until confluent, transferred to media containing 0.2% serum and incubated overnight before being exposed to 0 to 20 Gy of γ-irradiation from a ^{60}Co source, after which fresh media containing 0.2% serum was added. TGF-β1 (5 ng/ml) or vehicle control was added 24 hours later and the incubation continued for another 24 hours. Cells were scraped into RNeasy lysis thiocyanate (RLT) buffer (provided by the manufacturer) and RNA was isolated using a Midi RNeasy kit according to the manufacturer's protocol (Qiagen, Santa Clarita, CA). Other cells were treated identically and scraped into RIPA buffer for Western blot analysis.

Fibroblast Chemotaxis Assay

Cell migration studies were performed using a 48-well microchemotaxis chamber (NeuroProbe, Gaithersburg, MD). A 10-μm-pore size polycarbonate filter was immersed in a solution of 0.1 mg/ml of Vitrogen 100-purified collagen (Cohesion, Palo Alto, CA) and dried. Cells and chemotactic factors were diluted in Dulbecco's modified Eagle's medium/0.2% bovine serum albumin. Chemotactic factors, including assay buffer alone (negative control), 10 and 25 pg/ml of TGF-β1, and 10% serum (positive control) (27.5 μl) were placed in the lower compartment of the chamber, covered with the filter and 45 μl of cell suspensions (1×10^6 cells/ml) were pipetted into the upper chambers. After incubation at 37°C for 4 hours, the filter was removed, fixed in 100% methanol, and stained with Protocol (Biochemical Science, Swedesboro, NJ). Nonmigrated cells were wiped from the top side of the filter that was mounted on a microscope slide. Cells that had migrated to the underside of the filter were counted at ×200 magnification. For each experimental condition four to six wells were analyzed with data presented as mean number of cells per field ± SEM.

Western Blotting

Protein lysates (10 μg) were run on 10% Tris-glycine sodium dodecyl sulfate gels (Invitrogen, Carlsbad, CA) and transferred onto nitrocellulose membranes (Bio-Rad, Hercules, CA). After blocking in Tris-buffered saline/0.1% Tween-20/3% bovine serum albumin, membranes were incubated overnight with anti-smooth muscle actin (SMA) Ab-1 (Neomarkers, Fremont, CA) at 0.2 μg/ml in the same buffer. After washing, the blots were incubated for 1 hour in peroxidase-conjugated goat anti-mouse secondary antibody (0.16 μg/ml) from Jackson Immunoresearch Labs (West Grove, PA). Other blots were blocked with TBST/5% dry milk, probed overnight with anti-CTGF (kind gift of Dr. D. Abraham, London, UK) at a 1:1000 dilution and incubated for 1 hour with peroxidase-conjugated anti-rabbit IgG (Vector, UK) at a 1:2000 dilution. After additional washes the signal was detected using the Super Signal enhanced chemiluminescence kit from Pierce (Rockford, IL). Blots were reprobed using rabbit anti-actin(20-33) (Sigma Chemical) that recognizes all actin isoforms to confirm equal protein loading.

Northern Blotting

Total RNA (10 μg) was electrophoresed through a 1% agarose/formaldehyde gel containing ethidium bromide. After UV photography, RNA was transferred onto a Nytran membrane with buffer containing 1.5 M NaCl/0.1 M NaH_2PO_4/0.01 M EDTA using the Turboblotter method (Schleicher and Schuell, Keene, NH). The membrane was cross-linked with a UV Stratalinker (Stratagene, Menasha, WI). The CTGF vector containing a 1.5-kb CTGF insert cloned into the *Eco*RI/*Kpn*I site of pBluescript SK was provided by Dr. A. Holmes (Royal Free Hospital, London, UK). The TGF-β1 insert corresponded to the *Hind*III-*Xba*I fragment of rat TGF-β1.[25] cDNA insert (25 ng) was labeled with [α-^{32}P]dCTP by random priming performed according to Life Technologies (Rockville, MD) RTS labeling procedures. Blots were prehybridized, hybridized, and washed[26] before exposure to XAR-2 film. Densitometric scans of the films were quantitated with ImageQuant software. Data were normalized based on the intensity of the 18S and 28S RNA bands.

Quantitation of Wound Breaking Strength

Wound breaking strength was determined using the BTC-2000 Dynamic Skin Analyzer (SRLI Technologies, Nashville, TN). Mice were sacrificed immediately before analysis, shaved, and a 1-cm test chamber secured to the wound. Negative pressure was applied at a rate of 10 mmHg/second, increasing until the wound bursting point. Bursting strength (mean ± SEM) was measured 7 days after wounding on 8 to 18 wounds of each genotype from 11 WT or KO mice each having one to two wounds on the irradiated and nonirradiated flank.

Results

To model wounds made in skin of patients treated previously with radiation therapy, we made full-thickness incisions 6 weeks after irradiation of an isolated skin flap of mice with a single dose from an X-ray source.

Effects of Irradiation on Skin of WT and KO Mice

KO mice showed a scarred but completely healed epidermis 30 days after irradiation with a single 45-Gy dose (Figure 1B), whereas WT littermates showed severe injury to the skin and evidence of scabbing and moist desquamation (Figure 1A). Because of the severity of the injury to the skin of WT mice, the dose of radiation was reduced to 30 Gy, and the response to irradiation was monitored, so

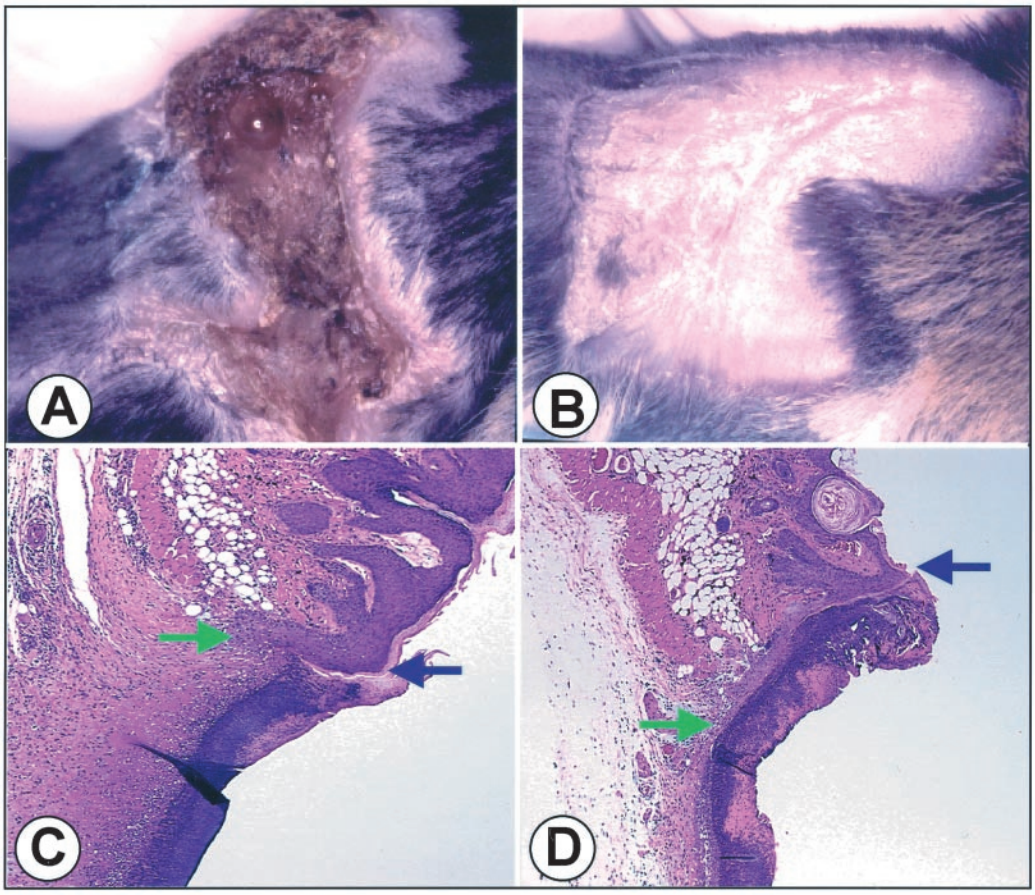

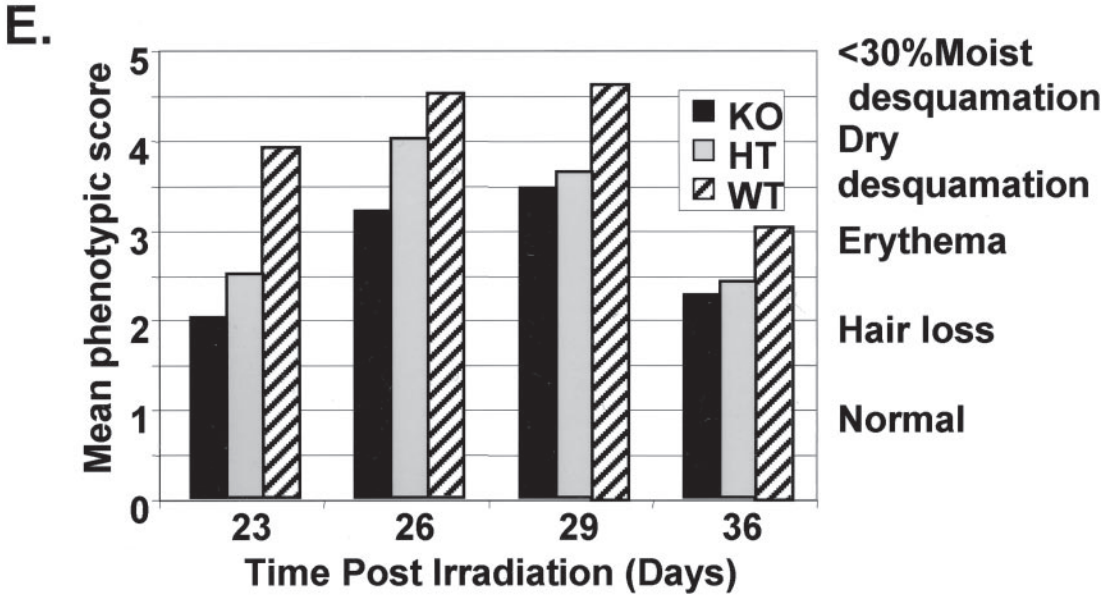

Figure 1. Smad3-null mice are resistant to the injurious effects of ionizing irradiation. **A** and **B:** Dramatic differences are apparent in the appearance of skin exposed to 45 Gy of ionizing radiation dependent on the Smad3 genotype at 30 days after irradiation. **C** and **D:** Histology of wounds 3 days after making 1-cm incisions in skin irradiated with 30 Gy 6 weeks before wounding as visualized by H&E staining. **Blue arrow** marks the edge of the wound; **green arrow** marks the edge of the migrating epithelial tongue. **A** and **C**, WT; **B** and **D**, KO. **E:** Phenotypic score[19] of effects of 30-Gy irradiation on flank skin of mice of different Smad3 genotypes. −/− (KO, **black bars**), +/− (HT, **gray bars**), and +/+ (WT, **striped bars**) mice were irradiated with 30 Gy as described. At the indicated time after irradiation, mice were evaluated for a skin reaction according to a phenotypic scale. 1, normal; 2, hair loss; 3, erythema; 4, dry desquamation; 5, <30% moist desquamation; 6, >30% moist desquamation. Values were averaged from 10 KO, 6 HT, and 9 WT mice scoring two irradiated flanks per mouse. Original magnifications, ×50.

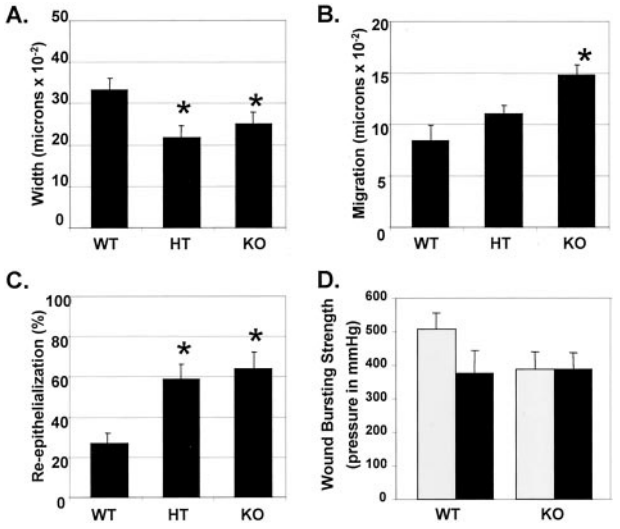

Figure 2. Smad3-null mice show a smaller wound width, accelerated epithelial migration, but reduced bursting strength compared to littermate controls. WT, HT, and KO mice were irradiated with 30 Gy and wounded as described. **A–C:** Three days after wounding, wounds were excised and samples were prepared as described. Wound width (**A**), epithelial migration (**B**), and the percent epithelialization (**C**) were determined as described in Materials and Methods. $n = 9$ to 13 wounds for each genotype for all measurements. *, $P < 0.05$ *versus* WT. **D:** Bursting strength of wounds in irradiated (30 Gy, **black bars**) or sham-irradiated (**gray bars**) skin was determined 7 days after wounding as described. $n = 8$ to 18 wounds analyzed.

that a time point for wounding could be chosen when healing of skin lesions was complete.

Erythema and hair loss result from radiation injury to the basal keratinocytes and hair follicle epithelium and from changes in the dermal vasculature resulting in influx of inflammatory cells and activation of immune cells. Depending on the extent of injury to the basal keratinocytes, this will progress to either dry desquamation in which remaining basal keratinocytes differentiate to corneal layer components, or to moist desquamation in which basal keratinocytes are lost and the dermis is exposed.[13] Onset of hair loss and erythema was delayed in skin of KO mice exposed to a single 30-Gy dose and the lesions did not progress to either the dry or moist desquamation seen in littermate WT mice (Figure 1E). Phenotypic scores[19] of HT mice fell between results obtained with WT and KO mice, suggesting that expression levels of Smad3 were directly related to the response. Based on these observations, mice were wounded 5 to 6 weeks after irradiation with 30 Gy, understanding that the model is complicated by the more favorable skin phenotype in KO mice at the time of wounding.

Re-Epithelialization of Wounded Irradiated Cutaneous Wounds

Histological examination of linear 1-cm incisional wounds of the irradiated flank 3 days after wounding showed that wounds in KO mice exhibited greater migration of the epithelial tongue (Figure 1, C and D) and were narrower, with a smaller area and reduced cellularity of granulation tissue compared to wounds in WT littermates. Wounds in either HT or KO mice were ~70% the width of wounds in WT littermates at 3 days after wounding (Figure 2A, $P < 0.05$). Epithelial migration was ~1.3- and 1.8-fold ($P < 0.05$) greater in KO mice compared to HT or WT littermates, respectively (Figure 2B) such that KO wounds were 64% re-epithelialized 3 days after wounding ($P < 0.05$), compared to 27% in WT littermates (Figure 2C). A comparative time-course analysis of wound closure in KO and WT mice showed that wounds in nonirradiated skin epithelialize more quickly than those in irradiated skin within the same genotype (data not shown). These data corroborate our previous findings[10] and suggest that the beneficial effects of loss of Smad3 for closure of wounds are retained in previously irradiated skin.

Table 1. Quantitative Analysis of Cellular Composition of the Granulation Tissue 3 Days after Wounding of Previously Irradiated Flank Skin Compared to Nonwounded, Irradiated Skin (in Parentheses)

	Number of cells/high-power field ± SEM		
	WT	HT	KO
Mast cells	24 ± 4 (22)*	ND	19 ± 3 (13)
Macrophages	31 ± 3 (17)	ND	28 ± 3 (9)
Neutrophils	64 ± 4† (8)	40 ± 4‡ (5)	31 ± 5 (4)
Myofibroblasts	38 ± 4† (16)	22 ± 1†‡ (13)	10 ± 1 (12)

*Numbers in parentheses are taken from Flanders et al[11] for nonwounded, irradiated skin.
†$P < 0.0001$ *versus* KO.
‡$P < 0.003$ *versus* WT.
ND, not determined.

Cellularity of Wounded Irradiated Tissue

The early stages of wound healing are characterized by active migration of macrophages, neutrophils, lymphocytes, and fibroblasts into the wound bed.[1] At 3 days after wounding, numbers of mast cells and macrophages per unit area of wound granulation tissue of irradiated KO mice were only slightly less than WT, being on average, 81 and 89% that of WT mice, respectively (Table 1). In contrast, there were highly significant ($P < 0.0001$) Smad3 dosage-dependent reductions in the number of neutrophils (KO 48% of WT) in the wound bed, although the fold-increase in neutrophils in the wound bed compared to surrounding, unwounded irradiated tissue was similar for all genotypes (approximately eightfold). For myofibroblasts, both the total number (KO 27% of WT) and the fold-increase compared to unwounded skin were dependent on the Smad3 dosage, with values for HT mice lying nearly midway between KO and WT. These differences are evident in sections of the wound bed stained to visualize neutrophils (Figure 3, A and B) and myofibroblasts (Figure 3, C and D). The overall reduced cellularity of the granulation tissue of the KO mice is also appreciated in these sections.

To ascertain whether the striking decrease in the number of myofibroblasts in the granulation tissue of wounds of the KO mice was because of decreased recruitment of fibroblasts into the wound bed or to a role for Smad3 in differentiation of fibroblasts to myofibroblasts, we treated primary neonatal dermal fibroblasts with TGF-β and as-

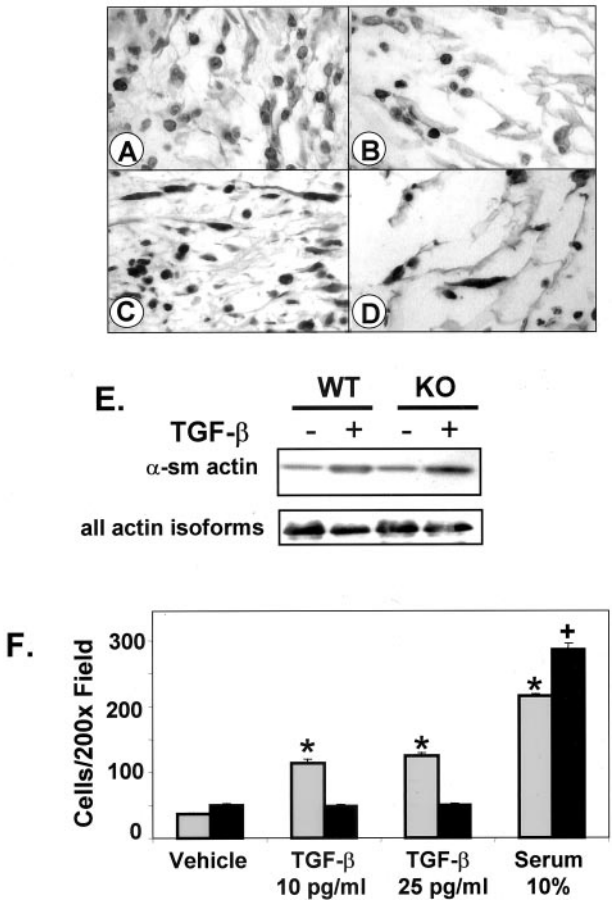

Figure 3. The number of neutrophils and myofibroblasts is significantly reduced in wounds of irradiated KO mice compared to WT. Sections from wounds in irradiated flank skin of WT (**A**, **C**) and KO (**B**, **D**) were stained with rat anti-mouse neutrophil antibody (**A**, **B**) or anti-α-SMA to identify myofibroblasts (**C**, **D**). Peroxidase, with Carazzi hematoxylin counterstain. **E:** Dermal fibroblasts prepared from WT or KO neonatal mice were treated with TGF-β1 (5 ng/ml) for 4 days. Cell lysates were subjected to Western blotting using anti-SMA or antibody that recognizes all actin isoforms as described in Materials and Methods. **F:** Smad3 WT fibroblasts (**gray bars**) migrate in response to TGF-β, whereas KO fibroblasts (**black bars**) do not. Results are representative of four experiments in which 3.2 to 3.8 times more WT fibroblasts migrated in response to TGF-β than to vehicle, whereas KO fibroblasts did not migrate in response to TGF-β, but did migrate toward 10% serum. $n = 4$ to 6 wells/treatment. *, $P < 0.0002$ *versus* WT, vehicle treated. $^{+}$, $P < 0.00007$ *versus* KO, vehicle treated. Original magnifications, ×400 (**A–D**).

sessed their expression of α-SMA. The ability of TGF-β to induce expression of α-SMA was independent of Smad3 (Figure 3E), consistent with a report demonstrating that either Smad2/4 or Smad3/4 complexes can stimulate the activity of the α-SMA enhancer element[27] and the finding that Smad2 is expressed at normal levels in KO mice.[23] Because fibroblasts respond chemotactically to TGF-β,[28] and because the chemotaxis of neutrophils,[23] macrophages, and keratinocytes[10] to TGF-β was shown to be Smad3-dependent, we examined the chemotaxis of primary WT and KO dermal fibroblasts to TGF-β (Figure 3F). KO fibroblasts showed a severely reduced chemotactic response to TGF-β (10 to 25 pg/ml)($P < 0.0002$), while they retained the ability to migrate toward a gradient of 10% serum ($P < 0.00007$ compared to vehicle). Together, these data suggest that recruitment of fibroblasts into the granulation tissue, rather than differentiation of fibroblasts to myofibroblasts is dependent on Smad3.

Bursting Strength of Wounds

Although more rapid epithelialization might increase wound bursting strength, the decreased cellularity of the granulation tissue and the presumed reduced extracellular matrix deposition by fibroblasts in wounds in KO mice might have the opposite effect. To address this, we measured the bursting strength of wounds made in the irradiated flanks of WT and KO mice, with contralateral sham-irradiated flanks serving as controls (Figure 2D). Bursting pressure (in mmHg)— a direct measurement of *in vivo* wound strength—was reduced ~25% by previous irradiation of the skin in WT mice, in agreement with a previous report.[17] This difference was not seen in wounds in KO mice, consistent with the reduced effects of irradiation on the skin of these mice. The bursting strength of wounds in KO mice was similar to that in irradiated WT mice.

Expression of TGF-β1 and CTGF Is Reduced in Wounds of KO Mice

We previously reported enhanced TGF-β1 staining in irradiated, unwounded WT compared to KO skin.[11] Consistent with impaired autoinduction of TGF-β1 in cells derived from KO mice,[10,29] immunohistochemical expression of TGF-β1 in the wound bed of irradiated WT skin (Figure 4, A and C) was significantly higher than in KO wounds, even though previous irradiation caused a slight increase in TGF-β1 staining in the wound bed in both genotypes, compared to wounds in contralateral unirradiated skin (Figure 4, B and D). To see whether this effect might also hold for other genes responsive to TGF-β and implicated in wound healing, we examined the expression of CTGF, a target of TGF-β in fibroblasts suggested to mediate its effects on collagen deposition.[30] CTGF staining was also stronger in the WT wound bed (Figure 4, E and G) as compared to the KO (Figure 4, F and H), but, like TGF-β, was increased in irradiated wounds of both genotypes (Figure 4; E to H).

Dermal Fibroblasts Derived from KO and WT Mice Show Different Responses to Irradiation and TGF-β

To address mechanisms underlying the enhanced expression of TGF-β1 and CTGF in irradiated wounds, we assessed induction of their mRNAs in primary fibroblasts treated with TGF-β1, irradiated with 5 Gy, or both with TGF-β1 added 24 hours after irradiation (Figure 5, A and B). Irradiation of the cells did not itself induce expression of TGF-β1, and had little effect on autoinduction of TGF-β1, independent of the genotype. The fold-induction by TGF-β was reduced in KO compared to WT cells, similar to the reduced autoinduction seen previously in KO macrophages[10] and mouse embryo fibroblasts.[29] In contrast,

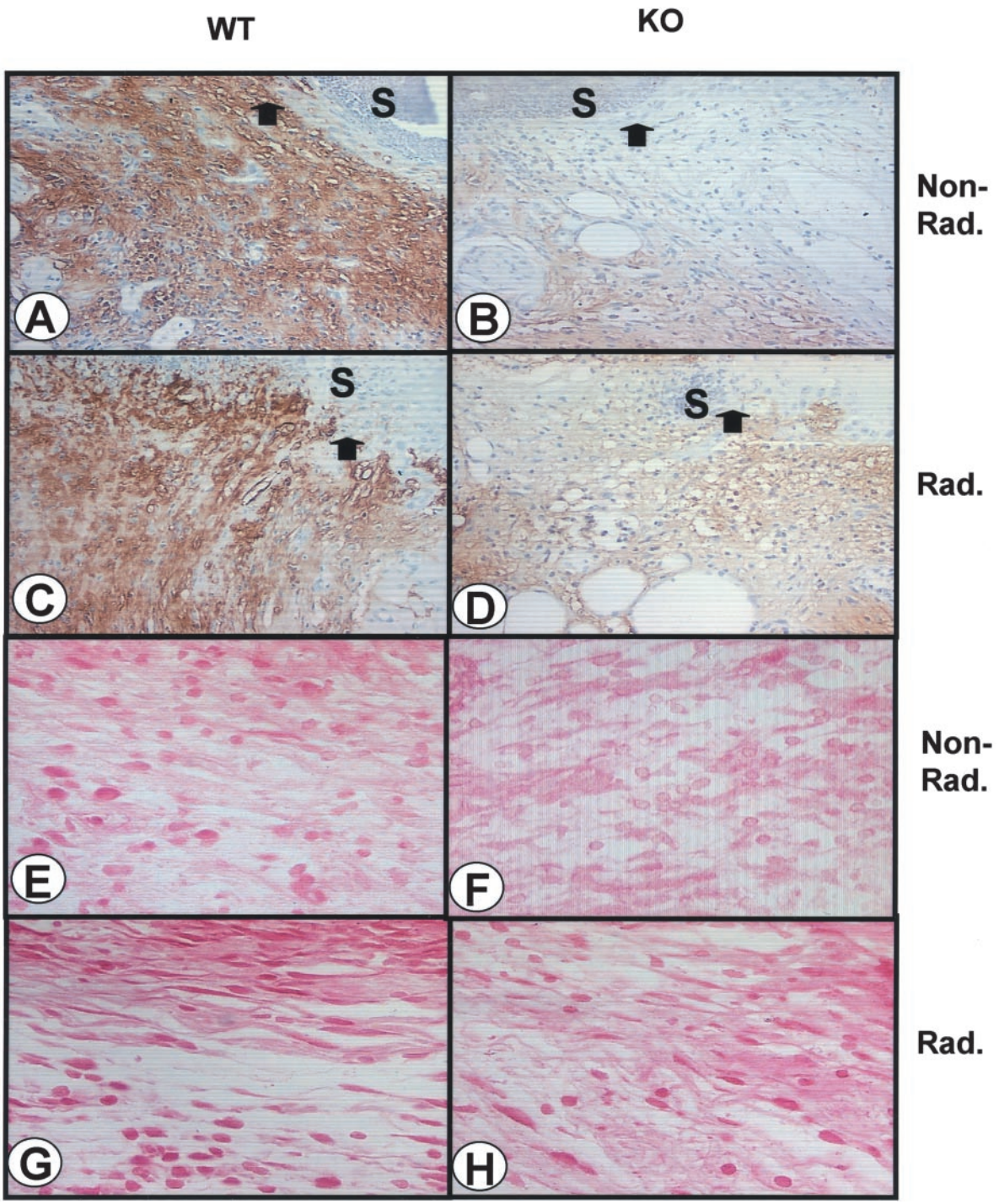

Figure 4. Levels of immunohistochemical staining for TGF-β and CTGF are higher in the granulation tissue of irradiated WT compared to KO wounds 3 days after wounding. Wound cross-sections from nonirradiated (**A**, **E**) and irradiated (**C**, **G**) WT and KO (**B** and **F, D** and **H**, respectively) mice were stained with antibodies against extracellular TGF-β1 (**A–D**) or CTGF (**E–H**) as described. **A–D** are ×200 magnification photographs taken immediately beneath the epithelium. The **arrow** marks the edge of the migrating epithelium and S marks the position of the scab. Peroxidase with Carazzi hematoxylin counterstain. **E–H** are ×400 magnification photographs taken deeper in the dermis at the edge of the wound bed. Red alkaline phosphatase.

although TGF-β enhanced expression of CTGF mRNA in both WT and KO fibroblasts, previous irradiation dose-dependently enhanced the induction of CTGF by TGF-β up to a maximum of threefold by 20 Gy in WT cells, with little effect on the response of the KO cells to TGF-β (Figure 5; A, C, and D). Western blotting of cells irradiated with 5 Gy confirmed the mRNA results (Figure 5E).

Loss of Smad3 Reduces Scarring

Scarring is related not only to the quantity of collagen produced, but to its quality as assessed by its organization and state of aggregation, which is a reflection of changes in dermal architecture and the presence of cells such as myofibroblasts.[22,31] Staining of histological sec-

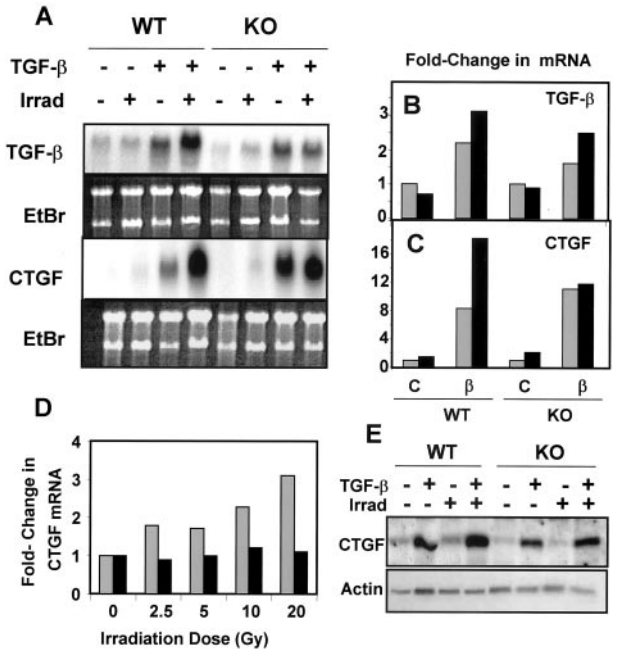

Figure 5. Irradiation augments the effects of TGF-β on autoinduction and induction of CTGF. Dermal fibroblasts prepared from WT or KO neonatal mice were subjected to 5 Gy of γ-irradiation (Irrad) followed 24 hours later by treatment with TGF-β1 as described in Materials and Methods. **A:** Northern blotting of RNA isolated from these cells using the indicated probe; **bottom** panel shows ethidium bromide staining of the gel. **B** and **C:** Fold-change in TGF-β or CTGF mRNA levels. For each genotype the level of hybridization of the nonirradiated, untreated cells was set to 1 and hybridization levels (normalized to correct for loading differences) were compared to these levels. No irradiation, **gray bars**; with irradiation, **black bars**. **D:** WT (**gray bars**) or KO (**black bars**) dermal fibroblasts were irradiated at the indicated doses followed 24 hours later by treatment with TGF-β. Northern blotting was performed on RNA prepared from these cells using a CTGF probe and data normalized to the nonirradiated sample for each genotype. **E:** Western blotting of lysates from dermal fibroblasts treated as indicated and probed with anti-CTGF or anti-actin.

tions with Picrosirius red and evaluation under polarized light provides a measure of the organizational pattern of collagen fibrils as well as their thickness.[31,32] Normal dermal architecture, similar in skin of WT and KO mice, is characterized by thin, weakly birefringent yellow-greenish fibers in a basketweave pattern (Figure 6, A and B, left of arrow). In contrast, 10 weeks after 30 Gy of irradiation, the dermis of unwounded WT (Figure 6C), but not KO skin (Figure 6D), was characterized by the prominent appearance of thicker collagen fibers with a orange-red birefringence suggestive of a scarring fibrosis. The scar index of unwounded WT irradiated skin was eightfold higher than KO (12.9 *versus* 1.6)—evidence that intrinsic differences in response to irradiation might contribute to the different wound phenotypes observed. Surprisingly, the scar index in the wound bed 5 weeks after wounding is similar in the WT and KO, irradiated and nonirradiated mice and not different from that of nonwounded skin (Figure 6), however the collagen architecture appears as a more parallel pattern in the irradiated WT skin (Figure 6C, inset) compared to the basketweave pattern in the other wounds (Figure 6; A, B, and D, insets).

Discussion

Although both Smad2 and Smad3 are phosphorylated directly by the TGF-β and activin type I receptors (ALK5 and ALK4, respectively), the selective DNA binding of Smad3, and not Smad2 likely underlies their distinct cellular targets and different requirements in embryogenesis.[29,33] TGF-β-dependent synthesis of collagens 1, 3, 6, and 7 and tissue-inhibitor of metalloproteinases-1 are Smad3-dependent,[34] as well as the more complex processes of TGF-β-dependent chemotaxis and inhibition of epithelial migration,[10] implicating this pathway in both wound healing and fibrosis. Other signaling pathways including phosphoinositol-3 kinase and the mitogen-activated protein kinases also mediate effects of TGF-β and activin on cells.[35] Based on the multiplicity of pathways involved, it is remarkable that elimination of only one specific signaling arm dependent on Smad3 can have such profound effects.

Because activin also signals through Smad3, some of the responses in the KO mouse may be because of altered activin signaling. Expression of endogenous activin is strongly up-regulated in skin after wounding and its overexpression in skin causes dermal fibrosis and epidermal hyperthickening.[36] Overexpression of the activin antagonist, follistatin, in skin delays wound healing, but reduces scarring,[37] suggesting that the reduced fibrosis and scarring in skin of irradiated KO mice could result from blocking Smad3-dependent signaling from not only TGF-β, but also activin.

Because Smad3 seems necessary for the TGF-β-dependent chemotaxis of neutrophils, macrophages, and fibroblasts into the wound bed[10,23] (Figure 3F), analysis of the cellularity of the wound bed of KO mice allows one to deduce whether migration of particular cells is dependent on TGF-β or on other signals. Thus whereas migration of macrophages into the wound bed in nonirradiated wounds was clearly Smad3-, and likely TGF-β/activin-dependent,[10,38] this difference is not seen in wounds made in irradiated skin (Table 1), suggesting that irradiation produces signals other than TGF-β that are capable of recruiting macrophages. For neutrophils, the absolute number but not the fold-increase in the wound bed compared to surrounding unwounded skin is dependent on the Smad3 genotype. In contrast, the recruitment of fibroblasts into wounds in irradiated skin is strongly dependent on Smad3/TGF-β/activin and likely contributes to the wound phenotype in KO mice, and to the reduced numbers of myofibroblasts in the wound bed. Resultant reduced levels of TGF-β in the skin and wounds of KO mice also likely contribute indirectly to the reduced numbers of inflammatory cells.[10,11]

Many of the effects of TGF-β on fibrosis are attributed to the profibrotic peptide, CTGF, a cysteine-rich mitogenic peptide belonging to the recently described CCN gene family of immediate early response genes.[30,39] Although Smad3 has been implicated in induction of CTGF expression by TGF-β in fibroblasts, other pathways including ras/MEK/ERK and protein kinase C also contribute and may, in certain instances operate independently of the Smad-binding site, as in the elevated expression of

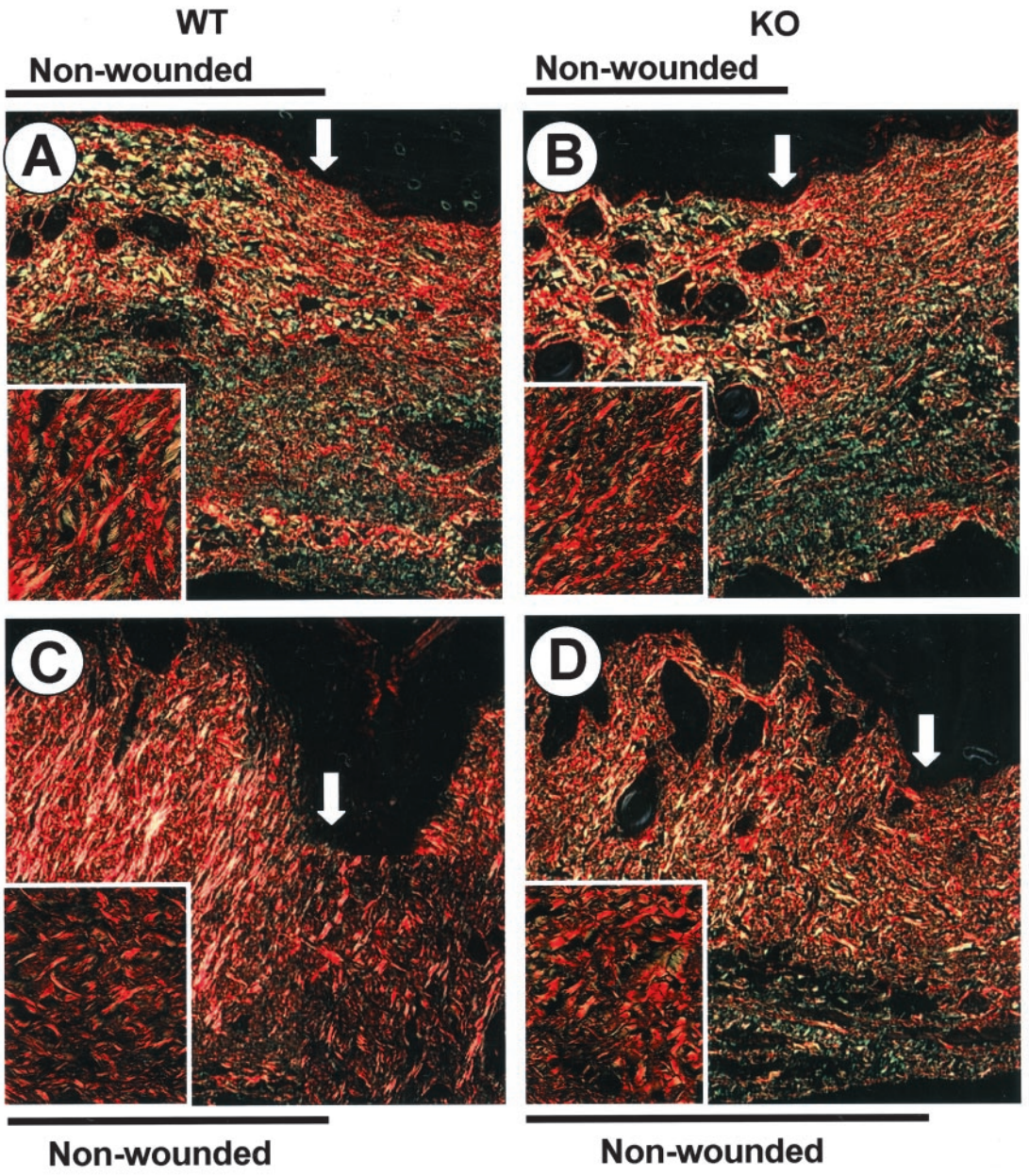

Scar Index ± SEM

	WT		KO	
	Wound Bed	Edge	Wound Bed	Edge
Non	1.5±0.1	2.7±1.0	1.8±0.8	1.9±0.5
Rad	1.5±0.4	12.9±5.7*	1.8±0.8	1.6±0.3

***p<0.03 vs wound bed of WT Rad, edge of WT Non, and edge of KO Rad**

Figure 6. Picrosirius-red staining shows similar matrix production in the wound bed of WT and KO mice 5 weeks after wounding, but a reduced scarring phenotype in the dermis at the wound edge of KO mice after irradiation. Skin sections from wounded, nonirradiated (**A**) and irradiated (**C**) WT and KO (**B** and **D**, respectively) mice were stained with Picrosirius red and photographed under polarized light. The **arrow** marks the edge of the wound. **Inset** is a higher magnification of the granulation tissue. Scar index as described in Materials and Methods; three to five wounds analyzed per treatment with two edge measurements, one on either side of the wound bed. *, $P < 0.03$ *versus* wound bed of WT Rad, edge of WT Non, and edge of KO Rad. Original magnifications: ×200 (**A–D**); ×400 (**inset**).

CTGF in scleroderma.[40,41] The strong activation of PKC isoforms and MEK/ERK by ionizing radiation[42] suggests that this could contribute to observed dose-dependent sensitization of CTGF induction by TGF-β in irradiated WT but not KO fibroblasts (Figure 4). The markedly reduced levels of TGF-β1 in injured or irradiated KO skin,[10] likely also contribute to the reduced levels of CTGF in KO wounds and indirectly to the reduced scarring and accumulation of collagen.

The increasing use of ionizing radiation for treatment of malignancy and its resultant unwanted acute and chronic effects on skin, makes study of wound healing in irradiated skin an important clinical problem. Surgery on previously irradiated skin poses problems based on the degree of radiation dermatitis, damage to the microvasculature, and possible complications of fibrosis, each of which is dependent, in part, on the radiation dosage and the timing of surgery after irradiation.[12,13] The desirable outcome of more rapid wound closure, reduced inflammation, and the potential for reduced scarring in irradiated skin of KO mice suggest that development of small molecule inhibitors of Smad3 may prove beneficial not only in protection from radiation injury, but also in the healing of surgical wounds in previously irradiated tissues. Importantly, wound width and extent of epithelialization appear to have a threshold requirement for Smad3 such that values for HT mice are not significantly different from KO (Figure 2, A and C), suggesting that even partial reduction of Smad3 levels might have a favorable clinical effect on certain wound parameters.

Acknowledgments

We thank Dr. Chuxia Deng for generously sharing the Smad3-null mice, Drs. Alan Holmes and David Abraham for providing CTGF Western blots and the CTGF plasmid, and Dr. Vincent Falanga for providing critical comments on the manuscript.

References

1. Roberts AB, Sporn MB: Transforming growth factor-β. The Molecular and Cell Biology of Wound Repair. Edited by RAF Clark. New York, Plenum Press, 1996, pp 275–308
2. Martin P: Wound healing—aiming for perfect skin regeneration. Science 1997, 276:75–81
3. Singer AJ, Clark RA: Cutaneous wound healing. N Engl J Med 1999, 341:738–746
4. Schmid P, Itin P, Cherry G, Bi C, Cox DA: Enhanced expression of transforming growth factor-beta type I and type II receptors in wound granulation tissue and hypertrophic scar. Am J Pathol 1998, 152:485–493
5. Frank S, Madlener M, Werner S: Transforming growth factors beta1, beta2, and beta3 and their receptors are differentially regulated during normal and impaired wound healing. J Biol Chem 1996, 271: 10188–10193
6. Sporn MB, Roberts AB, Shull JH, Smith JM, Ward JM, Sodek J: Polypeptide transforming growth factors isolated from bovine sources and used for wound healing in vivo. Science 1983, 219:1329–1331
7. Beck LS, DeGuzman L, Lee WP, Xu Y, McFatridge LA, Amento EP: TGF-beta 1 accelerates wound healing: reversal of steroid-impaired healing in rats and rabbits. Growth Factors 1991, 5:295–304
8. Beck LS, DeGuzman L, Lee WP, Xu Y, Siegel MW, Amento EP: One systemic administration of transforming growth factor-beta 1 reverses age- or glucocorticoid-impaired wound healing. J Clin Invest 1993, 92:2841–2849
9. Massague J, Blain SW, Lo RS: TGFbeta signaling in growth control, cancer, and heritable disorders. Cell 2000, 103:295–309
10. Ashcroft GS, Yang X, Glick AB, Weinstein M, Letterio JL, Mizel DE, Anzano M, Greenwell-Wild T, Wahl SM, Deng C, Roberts AB: Mice lacking Smad3 show accelerated wound healing and an impaired local inflammatory response. Nat Cell Biol 1999, 1:260–266
11. Flanders KC, Sullivan CD, Fujii M, Sowers A, Anzano MA, Arabshahi A, Major C, Deng C, Russo A, Mitchell JB, Roberts AB: Mice lacking Smad3 are protected against cutaneous injury induced by ionizing radiation. Am J Pathol 2002, 160:1057–1068
12. Tibbs MK: Wound healing following radiation therapy: a review. Radiother Oncol 1997, 42:99–106
13. Tokarek R, Bernstein EF, Sullivan F, Uitto J, Mitchell JB: Effect of therapeutic radiation on wound healing. Clin Dermatol 1994, 12: 57–70
14. Bernstein EF, Salomon GD, Harisiadis L, Talbot T, Harrington F, Russo A, Uitto J: Collagen gene expression and wound strength in normal and radiation-impaired wounds. A model of radiation-impaired wound healing. J Dermatol Surg Oncol 1993, 19:564–570
15. Bernstein EF, Harisiadis L, Salomon G, Norton J, Sollberg S, Uitto J, Glatstein E, Glass J, Talbot T, Russo A: Transforming growth factor-beta improves healing of radiation-impaired wounds. J Invest Dermatol 1991, 97:430–434
16. Nall AV, Brownlee RE, Colvin CP, Schultz G, Fein D, Cassisi NJ, Nguyen T, Kalra A: Transforming growth factor beta 1 improves wound healing and random flap survival in normal and irradiated rats. Arch Otolaryngol Head Neck Surg 1996, 122:171–177
17. Gorodetsky R, McBride WH, Withers HR: Assay of radiation effects in mouse skin as expressed in wound healing. Radiat Res 1988, 116: 135–144
18. Bernstein EF, Sullivan FJ, Mitchell JB, Salomon GD, Glatstein E: Biology of chronic radiation effect on tissues and wound healing. Clin Plast Surg 1993, 20:435–453
19. Randall K, Coggle JE: Expression of transforming growth factor-beta 1 in mouse skin during the acute phase of radiation damage. Int J Radiat Biol 1995, 68:301–309
20. Randall K, Coggle JE: Long-term expression of transforming growth factor TGF beta 1 in mouse skin after localized beta-irradiation. Int J Radiat Biol 1996, 70:351–360
21. Martin M, Lefaix J, Delanian S: TGF-beta1 and radiation fibrosis: a master switch and a specific therapeutic target? Int J Radiat Oncol Biol Phys 2000, 47:277–290
22. Martin M, Lefaix JL, Pinton P, Crechet F, Daburon F: Temporal modulation of TGF-beta 1 and beta-actin gene expression in pig skin and muscular fibrosis after ionizing radiation. Radiat Res 1993, 134:63–70
23. Yang X, Letterio JJ, Lechleider RJ, Chen L, Hayman R, Gu H, Roberts AB, Deng C: Targeted disruption of SMAD3 results in impaired mucosal immunity and diminished T cell responsiveness to TGF-beta. EMBO J 1999, 18:1280–1291
24. Duncan MR, Frazier KS, Abramson S, Williams S, Klapper H, Huang X, Grotendorst GR: Connective tissue growth factor mediates transforming growth factor-beta-induced collagen synthesis; down-regulation by cAMP. EMBO J 1999, 13:1774–1786
25. Qian SW, Kondaiah P, Roberts AB, Sporn MB: cDNA cloning by PCR of rat transforming growth factor beta-1. Nucleic Acids Res 1990, 18:3059–3059
26. Church GM, Gilbert W: Genomic sequencing. Proc Natl Acad Sci USA 1984, 81:1991–1995
27. Cogan JG, Subramanian SV, Polikandriotis JA, Kelm Jr RJ, Strauch AR: Vascular smooth muscle alpha-actin gene transcription during myofibroblast differentiation requires Sp1/3 protein binding proximal to the MCAT enhancer. J Biol Chem 2002, 277:36433–36442
28. Postlethwaite AE, Keski-Oja J, Moses HL, Kang AH: Stimulation of the chemotactic migration of human fibroblasts by transforming growth factor beta. J Exp Med 1987, 165:251–256
29. Piek E, Ju WJ, Heyer J, Escalante-Alcalde D, Stewart CL, Weinstein M, Deng C, Kucherlapati R, Bottinger EP, Roberts AB: Functional characterization of transforming growth factor beta signaling in Smad2- and Smad3-deficient fibroblasts. J Biol Chem 2001, 276: 19945–19953
30. Grotendorst GR: Connective tissue growth factor: a mediator of TGF-

beta action on fibroblasts. Cytokine Growth Factor Rev 1997, 8:171–179
31. Rabau MY, Hirshberg A, Hiss Y, Dayan D: Intestinal anastomosis healing in rat: collagen concentration and histochemical characterization by Picrosirius red staining and polarizing microscopy. Exp Mol Pathol 1995, 62:160–165
32. Andrade GB, Montes GS, Conceicao GM, Saldiva PH: Use of the Picrosirius-polarization method to age fibrotic lesions in the hepatic granulomas produced in experimental murine schistosomiasis. Ann Trop Med Parasitol 1999, 93:265–272
33. Weinstein M, Yang X, Deng C: Functions of mammalian Smad genes as revealed by targeted gene disruption in mice. Cytokine Growth Factor Rev 2000, 11:49–58
34. Verrecchia F, Chu ML, Mauviel A: Identification of novel TGF-beta/Smad gene targets in dermal fibroblasts using a combined cDNA microarray/promoter transactivation approach. J Biol Chem 2001, 276:17058–17062
35. Roberts AB, Piek E, Bottinger EP, Ashcroft G, Mitchell JB, Flanders KC: Is Smad3 a major player in signal transduction pathways leading to fibrogenesis? Chest 2001, 120:43S–47S
36. Munz B, Smola H, Engelhardt F, Bleuel K, Brauchle M, Lein I, Evans LW, Huylebroeck D, Balling R, Werner S: Overexpression of activin A in the skin of transgenic mice reveals new activities of activin in epidermal morphogenesis, dermal fibrosis and wound repair. EMBO J 1999, 18:5205–5215
37. Wankell M, Munz B, Hubner G, Hans W, Wolf E, Goppelt A, Werner S: Impaired wound healing in transgenic mice overexpressing the activin antagonist follistatin in the epidermis. EMBO J 2001, 20:5361–5372
38. Petraglia F, Sacerdote P, Cossarizza A, Angioni S, Genazzani AD, Franceschi C, Muscettola M, Grasso G: Inhibin and activin modulate human monocyte chemotaxis and human lymphocyte interferon-gamma production. J Clin Endocrinol Metab 1991, 72:496–502
39. Moussad EE, Brigstock DR: Connective tissue growth factor: what's in a name? Mol Genet Metab 2000, 71:276–292
40. Kucich U, Rosenbloom JC, Herrick DJ, Abrams WR, Hamilton AD, Sebti SM, Rosenbloom J: Signaling events required for transforming growth factor-beta stimulation of connective tissue growth factor expression by cultured human lung fibroblasts. Arch Biochem Biophys 2001, 395:103–112
41. Holmes A, Abraham DJ, Sa S, Shiwen X, Black CM, Leask A: Ctgf and smads, maintenance of scleroderma phenotype is independent of smad signaling. J Biol Chem 2001, 276:10594–10601
42. Abbott DW, Holt JT: Mitogen-activated protein kinase kinase 2 activation is essential for progression through the G2/M checkpoint arrest in cells exposed to ionizing radiation. J Biol Chem 1999, 274:2732–2742